Present Status of Integrated Performance Achieved in Tokamak Experiments and Critical Issues Towards DEMO Reactor

Yoshiteru Sakamoto[1], Kenji Tobita[2], Masanori Araki[3]

IFERC project team in the BA activities, JAEA, Naka, Ibaraki, 311-0193 JAPAN

JAEA, Naka, Ibaraki, 311-0193 JAPAN

IFERC project team in the BA activities, JAEA, Rokkasho, Aomori, 039-3212 JAPAN

(Received: 20 November 2009 / Accepted: 7 May 2010)

This paper reports the present status of the integrated performance achieved in tokamak experiments and critical issues towards DEMO reactor. The achieved integrated performance towards DEMO reactor is visualized using by introducing the radar-screen diagram with the normalized performance. The normalized plasma parameters foreseen in DEMO have been developed experimentally in world-wide, but the highly integrated performance and long sustainment have not yet been achieved. The main differences of physics requirements between ITER and DEMO provides the critical issues such as the capability for non-inductive current drive, power handling in edge and divertor, ELM mitigation and the controllability of self-organized system. Such critical issues towards DEMO should be addressed with attention to trade-off relationships.

Keywords: tokamak, DEMO reactor, integrated performance, trade-off relationship, critical issues

1. Introduction

Recent advanced tokamak experiments have achieved high fusion performances, e.g., fusion triple product $n\tau T$ = 1.53×10^{21} m^{-3}skeV [1] and the DT equivalent fusion gain Q_{DT}^{eq} = 1.25 [2]. Moreover, significant fusion power has been demonstrated by D-T burning plasma experiments in JET [3, 4] and TFTR [5, 6]. The ITER as the next step device will demonstrate the fusion burning with higher fusion gain of Q ~ 10, which provides the physics basis of burning plasma, including the behavior of energetic particles produced by fusion reaction and the effect of self-heating towards DEMO reactors. The design values of device size, plasma configuration, absolute performance and normalized performance for fusion reactors and ITER are compared in table 1 together with the best-achieved individual normalized parameters in present tokamak experiments [7, 8]. In the table, SlimCS is one of the examples of compact DEMO reactor design [9], and Model A is one of the examples of power plant design [10]. Although the best-achieved individual normalized parameters in the experiments exceed the requirements for DEMO and ITER steady-state scenario, there is no result of simultaneous achievement of these parameters. The future reactors actually require not only the fusion performance but also the integrated performance. Furthermore, it is important to demonstrate the highly integrated performance under the other reactor relevant conditions which are the operation region of q_{95} ~ 5, electron temperature nearly equal to ion temperature and low momentum input due to dominant alpha heating.

In order to visualize the achieved performance towards ITER or DEMO, we introduce radar-screen diagram as shown in figure 1, which is similar diagram shown in [11]. The each corner represents the following parameters with the full scale corresponding to the ITER steady-state operation scenario:

- HH_{98y2}: confinement enhancement factor over ELMy H-mode scaling,
- β_N: normalized beta,
- f_{BS}: bootstrap current fraction of plasma current,
- f_{CD}: non-inductive driven current fraction of plasma current,
- *fuel purity*: ratio of fuel ion and electron density,
- P_{rad}/P_{heat}: radiation fraction of heating power including alpha heating,
- n_e/n_{GW}: normalized electron density by Greenwald density limit.

Towards ITER steady-state operation and DEMO, high values of these parameters should be simultaneously sustained for a long time. For example, ITER steady-state operation scenario [12] foresees HH_{98y2} = 1.61, β_N = 2.93, f_{BS} = 0.46, f_{CD} = 1.0, *fuel purity* of 0.82, f_{rad} = 0.53 and n_e/n_{GW} = 0.78. However present devices have never demonstrated such an integrated performance even with transient condition. It should be emphasized that even larger values of β_N, f_{BS} and f_{rad} are required for SlimCS.

This paper summarizes the present status of the integrated performance achieved in the present tokamak experiments and the critical issues towards a DEMO

author's e-mail: sakamoto.yoshiteru@jaea.go.jp

	Parameters	Reactor Design		ITER			Achieved values in experiments
		Slim CS (DEMO)	Model A (Power Plant)	Inductive	Steady state Scenario 4	Steady state Scenario 6	
Size & Configuration	Major radius, R_p (m)	5.5	9.55	6.2	6.35	6.35	3.56 (JT-60U), 2.91 (JET)
	Minor radius, a (m)	2.1	3.18	2	1.85	1.85	1.05 (JT-60U), 0.96 (JET)
	Aspect ratio, A	2.6	3	3.1	3.43	3.43	
	Elongation, κ_{95}	2	1.7	1.7	1.85	1.86	
	Triangularity, δ_{95}	~0.35	0.25	0.33	0.4	0.41	
	Safety factor, q_{95}	5.4		3	5.3	5.4	2.1 (DIII-D), 2.2 (JT-60U), 2.3 (JET)
	Plasma Volume (m^3)	941		831			~90 (JT-60U)
	Toroidal magnetic field, B_t / B_{max} (T)	6 / 16.4	7 / 13.1	5.3 / 11.8	5.18 / 11.8	5.18 / 11.8	8 (C-Mod), 4.8 (JT-60U
	Plasma current, I_p (MA)	16.7	30.5	15	9	9	4.5 (JET), 5.0 (JT-60U)
Absolute Performance	Electric output, Pe (Gwe)	1	1.55				
	Fusion output, P_{fus} (MW)	2950	5000	400	356	340	16 (JET), 10.7 (TFTR)
	Fusion gain, Q	≥ ~30	20	10	6	5.7	0.8 (JET), 1.25 [DT equ] (JT-60U)
	Heating power (α + external), P_{heat} (MW)	650-690		120	130.2	128	40 (JT-60U), 39.5 (TFTR)
	Current drive power, P_{CD} (MW)	60-100	246	40			
	Ion temperature, vol-ave. / central (keV)	17 / 28	22 / 23	8.0 / 19	12.5 / 25.0	12.1 / *	Ti(0)= 45 (JT-60U), 39 (JET)
	Ele. temperature, vol-ave. / central (keV)	17 / 28	22 / 23	8.8 / 23	12.3 / *	13.3 / *	Te(0)=26 (JT-60U)
	Ele. density, vol-ave. / central (E20/m^3)	1.1 / 1.7	1.1 / *	1.01 / 1.05	0.67	0.65	
	Stored Energy (thermal / fast-ion) (MJ)	942 / 299		320 / 32	287 / *	287 / *	Wth= 12.9 (JET), 10.9 (JT-60U)
Normalized Performance	Confinement improvement, HH_{y2}	1.3	1.2	1	1.57	1.61	2.3 (JT-60U)
	Normalized beta, β_N	4.3	3.5	1.8	2.95	2.93	4.5 (DIII-D), 4.8 (JT-60U)
	Bootstrap current fraction, f_{BS}	~0.75	0.45	0.15	0.481	0.463	>0.9 (JT-60U), 0.85 (DIII-D)
	Non inductive CD fraction, f_{CD}	1	1	0.21	1	1	1.0 (JT-60U, DIII-D)
	Normalized density, n_e/n_{GW}	0.98	1.2	0.85	0.82	0.78	1.4 (DIII-D), 1.7 (JT-60U)
	Radiation power fraction, P_{rad} / P_{heat}	~0.9			0.53	0.53	>1 (JT-60U)
	Fuel purity, n_{DT} / n_e	0.84					
	He fraction, f_{He}	0.05			0.041	0.04	
	Ar fraction, f_{Ar}	0.0023			0.0026	0.002	
	Be fraction, f_{Be}				0.02	0.02	
	H89	2.59					3.8 (JT-60U)

Table 1. Comparison of design parameters of Reactor design, ITER and the achieved values in experiments.

reactor.

2. Present status of integrated performance

2.1 Transient condition

Major examples of highly integrated performance achieved in transient condition are shown in figure 2. Note that the full scale of radar-screen represents the design values of SlimCS. One example is the result from DIII-D discharge (#122004) [13], which is one of the best-integrated performances achieved in the world-wide experiments towards steady-state tokamak operation scenario. The discharge condition at t = 2.0s is as follows: plasma current I_p ~ 1.35 MA, toroidal magnetic field B_T ~ 1.7 T, safety factor at the 95% flux surface q_{95} ~ 5.0, elongation κ ~ 1.9 and triangularity δ ~ 0.8, where strong plasma shaping was adopted in order to maximize the beta limit. Note that available operation range of DIII-D shaping are normally $1.0 < \kappa < 2.5$ and $\delta < 0.85$. In the discharge, the plasma current ramp-up and the toroidal magnetic field ramp-down are used to sustain the broader q-profile with reversed magnetic shear and high beta. Therefore the plasma performance is basically transient, but $\beta_N \sim 4$, $q_{min} \sim 2$ and $H_{89} \sim 2.5$ have been simultaneously sustained for almost 2 s. Here H_{89} is the confinement enhancement factor over L-mode scaling and q_{min} is minimum value of safety factor profile. Furthermore, high $f_{BS} \sim 60\% - 80\%$ and $f_{CD} \sim 100\%$ were transiently obtained. One of the key features for obtaining high beta is attributed to produce broader pressure profile. In the discharge, no internal transport barrier (ITB) in electron temperature profile is observed while clear ITBs in electron density and ion temperature profiles. The combination of these profiles avoids a large local pressure gradient. Furthermore, multiple feedback controls are essential for sustaining high performance, including feedback control of the n=1 error field and resistive wall mode (RWM) using both external and internal sets of n=1 magnetic coils, feedback control of β_N using the neutral beam injection (NBI), and feedback

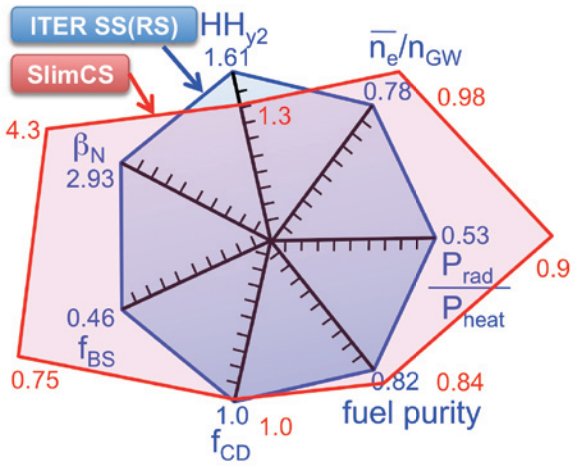

Fig.1 Comparison of the integrated plasma performance requirements foreseen in ITER steady-state operation scenario and SlimCS operation scenario using radar-screen with seven corners.

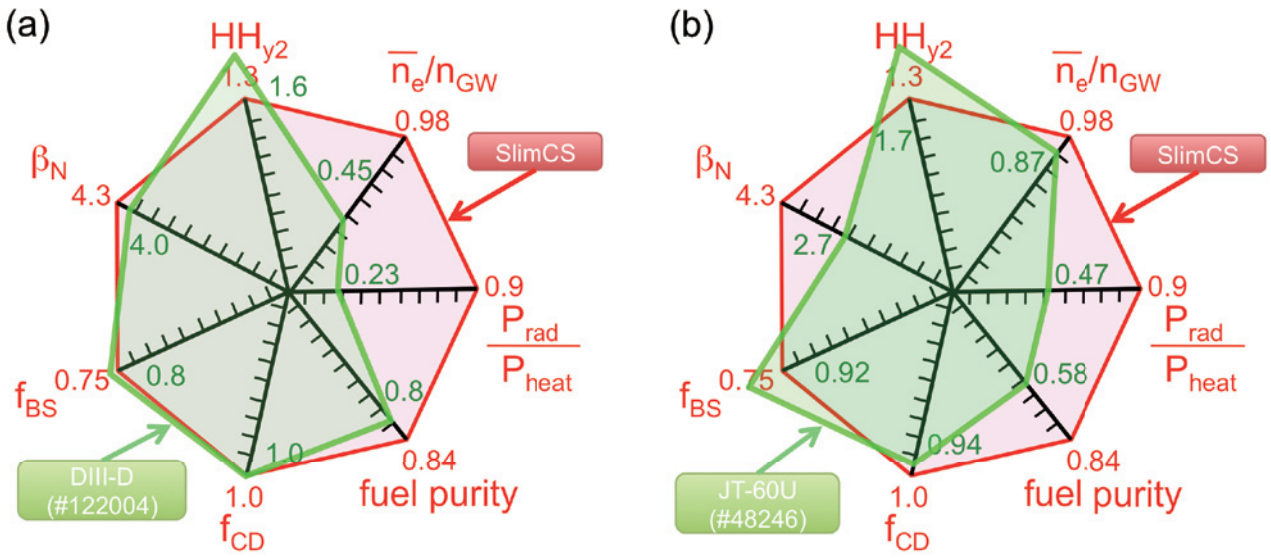

Fig. 2 Highly integrated performances achieved in transient condition. Comparisons of design values of SlimCS, as full scale in radar-screen with seven corners, and (a) DIII-D discharge (#122004) [13], (b) JT-60U discharge (#48246) [14].

control of the electron density using gas-puff. Although this discharge has largely succeeded in HH_{98y2}, β_N, f_{BS}, f_{CD} and fuel purity, as shown in figure 2(a), the remaining issues are higher n_e/n_{GW} and higher P_{rad}/P_{heat} under the trade-off relationships that are discussed in section 3.

Another example is the result from JT-60U discharge (#48246) [14], as shown in figure 2(b). The discharge condition is as follows: $I_p = 0.8$ MA, $B_T = 2.0$ T, $q_{95} \sim 5.3$, $\kappa \sim 1.5$ and $\delta \sim 0.37$. In the discharge, maximum performance was obtained just before the disruption due to the destabilization of RWM. Therefore the achieved performance is transient, but best integrated performance in JT-60U. The operation region of q_{95} is close to the design parameter of DEMO. Furthermore, the discharge was produced by the low momentum input condition expected in DEMO and electron temperature nearly equal to ion temperature, which conditions are expected in DEMO or a burning plasma. The high values of $HH_{98y2} \sim 1.7$, $\beta_N \sim 2.7$, $f_{BS} \sim 0.92$, $f_{CD} \sim 0.94$ and n $n_e/n_{GW} \sim 0.87$ are simultaneously achieved under the DEMO relevant plasma condition. The key features of the discharge are high confinement and high beta above no-wall beta limit. High confinement property is due to the strong ITB formation where the thermal diffusivities decreased to the neoclassical predicted level. Thanks to the wall stabilization, beta limit is significantly improved by factor of ~1.5. Since the disruption was occurred when the toroidal rotation velocity at q=3 surface decreased to the critical toroidal rotation velocity, the feedback control of toroidal rotation is required for the avoidance of the disruption. Although this discharge has largely succeeded in HH_{98y2}, f_{BS}, f_{CD} and n_e/n_{GW}, as shown in figure 2(b), the remaining issues are higher β_N, fuel purity, and P_{rad}/P_{heat} under the trade-off relationships that are discussed in section 3.

The typical characteristics of the reversed shear plasma are high confinement property and high f_{BS} due to the formation of ITB, while beta limit without wall stabilization is lower than positive (or weak) shear plasmas. Significant improvement of beta limit could be achieved by wall stabilization with keeping high confinement property. Therefore the reversed magnetic shear plasma with wall stabilization is one of the candidates for DEMO operation scenario, but long sustainment is one of the big issues. Main differences in the integrated performance between two cases shown in figure 2 are β_N and n_e/n_{GW}, which are attributed to the difference of ITB characteristics. As mentioned above, broader pressure profile was produced in DIII-D discharge while local steep pressure gradient in JT-60U. Therefore beta limit with wall stabilization in DIII-D discharge is higher than JT-60U. On the contrary, the normalized electron density in JT-60U is higher than DIII-D.

2.2 Quasi-steady state condition

Major examples of highly integrated performance achieved in quasi-steady state condition are shown in figure 3. One is the weak shear plasma and another is the reversed shear plasma, which are the results from JT-60U discharges (#35715 for the weak shear plasma and #43046 for the reversed shear plasma). In the case of the weak shear plasma one of the difficulties to obtain quasi-steady state condition is avoidance of the destabilization of neoclassical tearing modes (NTMs) that determine the beta limit of weak positive shear plasma. The highly integrated performance of the weak shear plasma without NTMs is shown in figure 3(a) [11, 15]. The discharge condition is as follows: $I_p = 1.5$ MA, $B_T = 3.7$ T, $q_{95} \sim 4.7$, $\kappa \sim 1.5$ and $\delta \sim$

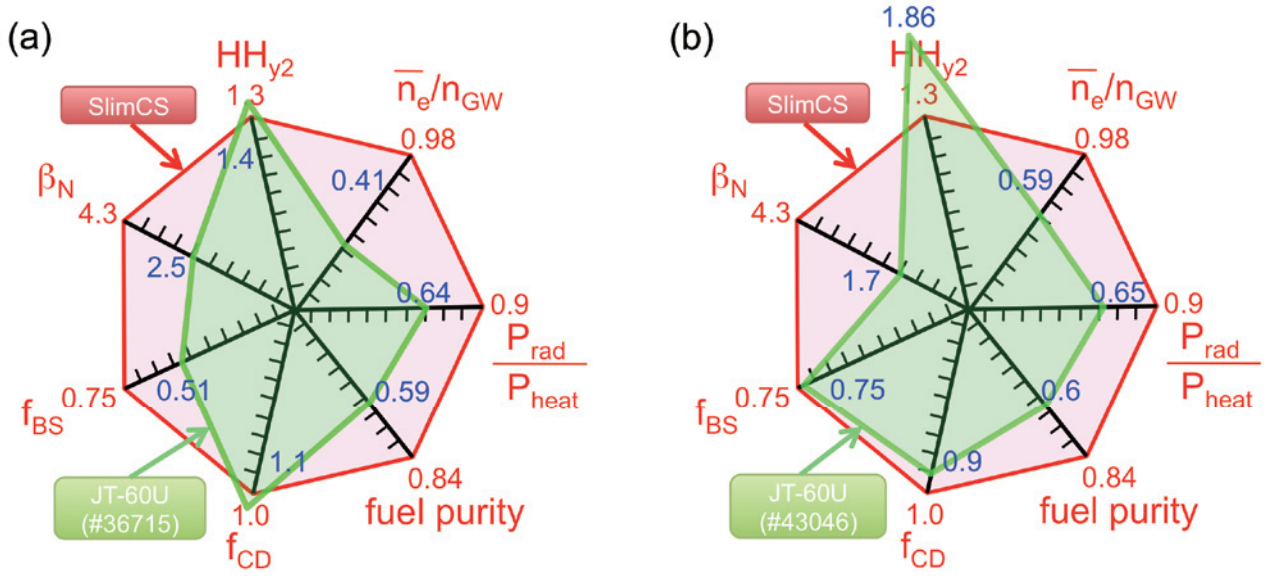

Fig. 3 Highly integrated performances achieved in quasi-steady state condition. Comparisons of design values of SlimCS, as full scale in radar-screen with seven corners, and (a) JT-60U weak shear discharge (#36715) [11, 15], (b) JT-60U reversed shear discharge (#43046) [17].

0.35. In the discharge, negative ion based neutral beam with a beam energy of 360 keV was injected in order to increase f_{CD}, and the stored energy feedback control was applied to keep a constant β_N below the NTM destabilization level. The high values of $HH_{98y2} \sim 1.4$, $\beta_N \sim 2.5$, $f_{BS} \sim 0.51$ and $f_{CD} \sim 1.1$ are simultaneously achieved. However the degree of attainment of β_N, f_{BS}, fuel purity, P_{rad}/P_{heat} and n_e/n_{GW} is roughly a half of design requirement of SlimCS.

In the case of the reversed shear plasma one of the difficulties to obtain quasi-steady state condition is avoidance of disruption due to the lower beta limit without wall stabilization. In addition, the reversed shear q profile gradually changes towards the stationary condition, where the value of q in core plasma region, including q_{min} and its location, decreases continuously due to the penetration of inductive field. Therefore the value of q_{min} passes through integer values until reaching stationary condition. Then the discharges frequently terminate by disruption when q_{min} goes across the integer values. In order to avoid disruptions, the pressure gradient at the ITB should be decreased when the plasma becomes unstable. The technique of the control of the ITB strength was developed in JT-60U reversed shear discharges by the control of toroidal rotation [16]. Long sustainment of the reversed shear plasma with high f_{BS} under nearly full non-inductive current drive condition was demonstrated in JT-60U by the toroidal rotation control to avoid a disruption. The discharge condition of the quasi-steady state reversed shear plasma shown in figure 3(b) is as follows: $I_p = 0.8$ MA, $B_T = 3.4$ T, $q_{95} \sim 8.3$, $\kappa = 1.6$, $\delta = 0.42$ [17]. Utilizing the feedback control of the stored energy by the perpendicular NBIs, $\beta_N \sim 1.7$ ($\beta_p \sim 2.4$) was maintained for 7.4 s. The high HH_{98y2} of ~ 1.9 was also maintained thanks to ITBs at $n_e/n_{GW} \sim 0.6$. Moreover, $f_{CD} > 0.9$ and $f_{BS} \sim 0.75$ were achieved. In this discharge, toroidal rotation control for pressure gradient control was applied at q_{min} being 4, and then the disruption was successfully avoided. The sustained duration of 7.4 s corresponds to $\sim 16\ \tau_E$ and $\sim 2.7\ \tau_R$. Here τ_E and τ_R are energy confinement time and current diffusion time, respectively. At the stationary phase, the profile of measured total current density agrees closely with that of non-inductive current density, which implies the plasma approached the stationary condition. The degree of attainment for the requirement of SlimCS is roughly over 70% except β_N.

2.3 Long pulse condition

The typical example of long sustained plasmas is shown in figure 4, which is the result from JT-60U discharge (#48158) [18] as the demonstration of ITER hybrid scenario. The discharge condition is as follows: $I_p = 0.9$ MA, $B_T = 1.54$ T, $q_{95} \sim 3.2$, $\kappa \sim 1.4$ and $\delta \sim 0.32$. In the discharge, long-pulse of NBI was injected for 30 s, and then $\beta_N > 2.6$ was sustained for 28 s. Furthermore, $HH_{98y2} > 1$ characterized by the peaked pressure profile was also sustained for 25 s, which corresponds to $\sim 14\ \tau_R$. Although sustainment of ITER hybrid operation scenario discharge is easier than steady-state operation scenario discharge, the achieved integrated performance is almost a half of the requirement for SlimCS, as shown in figure 4. In other words, the present status of integrated performance of the reliable operation scenario for long pulse operation hovers at a half level of the requirement for SlimCS.

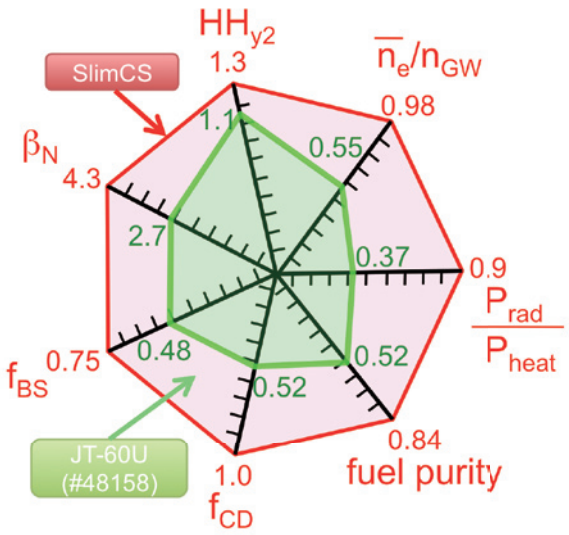

Fig. 4 Comparison of Integrated performance between SlimSC and JT-60U long pulse operation similar to ITER hybrid scenario [18].

3. Critical issues towards DEMO

Major critical issue for core plasma physics towards DEMO is the optimization of operation scenario for establishment of the highly integrated performance under the several trade-off relationships between parameters. The achieved highly integrated performances shown in this paper are mainly caused by core-plasma physics issues, not by the limit of the performance in engineering components. Therefore three types of trade-off issues for core-plasma physics are presented in this section. It should be noted, however, that the enhancement of capability of engineering components would contribute to improve the normalized parameters, for example, divertor pumping for fuel purity and current drive power for f_{CD}. In addition, since a DEMO reactor is generally positioned as a single step between ITER and a commercial reactor, the critical issues provided by the main differences of physics requirements between ITER and DEMO are also described in this section.

Although high-density operation is one of the major requirements for a DEMO plasma as shown in Table 1, degradation of confinement property was observed in the high-density experiments with large amount of particle fueling by gas puffing. Therefore first trade-off issue is the compatibility of high-density operation with keeping the high confinement. The presumed cause of the confinement degradation is the decrease in temperature at the peripheral region, which causes the decrease in temperature at the core due to profile stiffness nature, with increasing density under the pressure constant due to edge stability limit. Two ways solving the confinement degradation were demonstrated so far. One is the improvement of edge stability by increase of triangularity [19]. Although the confinement in the case of constant triangularity was degraded with increasing density, the confinement at constant density was improved by higher triangularity. As the result, higher confinement (HH_{98y2}~1) at high density (n_e/n_{GW}~1) was obtained at high triangularity of ~ 0.4. The other is use of central fueling by pellet injection [20]. Peaked density profile in the pellet injected discharge was obtained with keeping peripheral temperature at high level, while broad density profile and lower temperature in the gas-fueled discharge. In addition to these ways, the formation of ITB for electron density can access the high-density regime with high confinement. Actually, DEMO relevant high-density regime (n_e/n_{GW}~1) with high confinement (HH_{98y2}~1.3) was demonstrated only in reversed shear plasmas with strong ITB [21].

Second trade-off issue is simultaneous achievement of high beta and high confinement, because the reduced transport produces the steep pressure gradient while that reduces the beta limit. In general, the confinement in the reversed shear plasmas is higher than that in the weak shear plasmas, while the beta limit without conductive wall in the reversed shear plasmas is lower than that in weak shear plasmas. Best combination of the current and the pressure profiles for DEMO should be identified, because the combination mainly determines the beta limit. Strong candidate of the combination is weakly reversed magnetic shear as current profile, and moderate pressure gradient at the ITB and wide its location. Furthermore, wall stabilization by conductive wall is remarkably effective to achieve high beta with high confinement. Actually, DEMO relevant high beta (β_N~4.3) with high confinement (HH_{98y2}~1.3) was demonstrated in reversed shear plasmas with wall stabilization shown in Fig. 2 (a).

Enhancement of radiation fraction by impurity seeding is necessary for reducing heat load on plasma facing components. However, penetration of impurity into the core region degrades the fuel purity. Therefore, compatibility of high radiation fraction and fuel purity should be considered as third trade-off issue. Towards solving the issue, development of feedback control of radiation fraction through the impurity seeding is necessary to avoid the penetration, where large capability of pumping system is required. Recent experiments shows that the distribution of the radiation in the peripheral and divertor regions can be controlled by multi-impurity seeding technique [22], which would be useful for solving the issue.

In addition to above trade-off issues, critical issues towards DEMO based on the main differences of physics requirements between ITER and DEMO are summarized as follows.

(i) Long pulse operation (SlimCS: steady state, ITER: ~7min):

Steady-state operation requires sufficient capability for current drive including external driven current and bootstrap current. Appropriate plasma operation scenario

with high f_{BS} should be developed with high stability of the discharge. The profile of driven current should be compatible with the envisaged current profile such as weakly reversed magnetic shear.

(ii) Large fusion output (SlimCS: ~3GW, ITER: 0.5GW):

Although major radius and plasma volume of SlimCS are similar to those of ITER, fusion output of SlimCS is six times higher than that of ITER. This leads to large heat load to plasma facing components, which requires strong radiative edge and divertor, and ELM mitigation. Moreover, compatibility of plasma and DEMO relevant materials is also important.

(iii) High fusion gain (SlimCS: >20, ITER: 5-10):

The plasma with high fusion gain is characterized by self-organized system. In this system, current, pressure and rotation profiles are linked each other. Current profile is almost determined by self-generated bootstrap current. Heating profile is almost determined by alpha-heating. Rotation profile is almost determined by spontaneous rotation due to low momentum input. Therefore less controllability is expected. We should optimize actuators and diagnostics for control of self-organized plasma.

4. Conclusion

The normalized plasma parameters foreseen in DEMO have been developed experimentally in world-wide, but the integrated performance and long sustainment have not yet been achieved with the DEMO relevant material combinations. The large gaps between the DEMO parameters and the integrated performance in present experiments remain mostly in β_N, f_{BS}, n_e/n_{GW}, fuel purity and P_{rad}/P_{heat}. Furthermore, the main differences of physics requirements between ITER and DEMO provide the critical issues such as capability for non-inductive current drive, power handling in edge and divertor, ELM mitigation and controllability of self-organized system. Such critical issues towards DEMO should be addressed with attention to issues of trade-off relationships.

References

[1] S. Ishida *et al.*, *Proc. 16th Int. Conf. Plasma Physics and Controlled Nuclear Fusion Research*, Monteal, Canada, October 7-11, 1996, Vol. 1, p. 315, International Atomic Energy Agency (1997).

[2] T. Fujita *et al.*, Nucl. Fusion **39**, 1627 (1999).

[3] JET Team, Nucl. Fusion **32**, 187 (1992).

[4] A. Gibson and the JET Team, Phys. Plasmas **5**, 1839 (1998).

[5] J. D. Strachan *et al.*, Phys. Rev. Lett. **72**, 3526 (1994).

[6] R. J. Hawryluk *et al.*, Phys. Rev. Lett. **72**, 3530 (1994).

[7] V. Mukhovatov *et al.*, Nucl. Fusion **47**, S404 (2007).

[8] Y. Kamada *et al.*, J. Plasma Fusion Res. **81**, 849 (2005).

[9] K. Tobita *et al.*, Nucl. Fusion **49**, 075029 (2009).

[10] D. Maisonnier *et al.*, Nucl. Fusion **47**, 1524 (2007).

[11] Y. Kamada and the JT-60 team, Nucl. Fusion **41**, 1311 (2001).

[12] Plasma Performance Assessment 2004 section 3.4, ITER Technical Basis ITER EDA Documentation Series.

[13] A. M. Garofalo *et al.*, Phys. Plasmas **13**, 056110 (2006).

[14] Y. Sakamoto *et al.*, Nucl. Fusion **49**, 095017 (2009).

[15] A. Isayama *et al.*, Nucl. Fusion **41**, 761 (2001).

[16] Y. Sakamoto *et al.*, Nucl. Fusion **41,** 865 (2001).

[17] Y. Sakamoto *et al.*, Nucl. Fusion **45**, 574 (2005).

[18] N. Oyama *et al.*, Nucl. Fusion **49**, 065026 (2009).

[19] J. Ongena *et al.*, Nucl. Fusion **44,** 124 (2004).

[20] Y. Kamada *et al.*, Plasma Phys. Contrl. Fusion **44**, A279 (2002).

[21] Y. Sakamoto *et al.*, Plasma and Fusion Res. 5, S1008 (2010).

[22] N. Asakura et al., Nucl. Fusion 49, 115010 (2009).